Electric Field Calculation Based on PIDC in Monocomponent Development Systems

Jang Yi and Richard B. Wells
University of Idaho, Moscow, Idaho

Tom Camis
Hewlett Packard Company, Boise, Idaho

Abstract

Conventionally, electric fields in a development nip are often calculated for well-defined patterns (solid areas and isolated lines) or for a given charge distribution on the photoconductor surface. We propose an alternative method for field calculation based on various physical parameters of the development system. It uses a set of laser and photoconductor parameters to compute the exposure energy on the photoconductor surface, and the corresponding photoconductor surface potential is obtained from the Photo-Induced Discharge Characteristics (PIDC) of the photoconductor. The surface potential is then used as a boundary condition for solving Poisson's equation. The normal and horizontal fields are subsequently obtained by taking the negative gradient of the voltage. This method accounts for what is commonly known as dot-overlapping. Thus, electric fields anywhere in the gap for an arbitrary input bitmap can be calculated. Using our field model, simulation results from various input patterns are presented.

Introduction

Electric fields play a fundamental role in electrophotography. Variations in electric field separate photo-generated electron-hole pairs, affect surface potential, and transfer toner particles. Various field calculation methods have been proposed.[1-3] These methods are restricted to isolated lines or require knowledge about charge distribution on the photoreceptor surface. Our proposed method takes into account the physical parameters of a printer and calculates the electric field for any input bitmap.

Exposure and PIDC

Exposure seen at point (x, y) on the photoreceptor surface as a function of time from the moment the laser turns can be calculated.[4,5] Once exposure is obtained, knowledge of how exposure and voltage interact with each other can be utilized in obtaining the photoreceptor surface potential. The relationship between exposure and voltage is called the Photo Induced Discharge Characteristics (PIDC). The PIDC of a printer family is obtained from physical measurements.

A curve fit method using the simplex algorithm is employed to approximate the voltage at an arbitrary exposure level. Note that the surface potential obtained in this manner does not account for the effect of an electrode. In fact, when an electrode is brought in from infinity, the surface potential changes. This potential change is discussed in the next section.
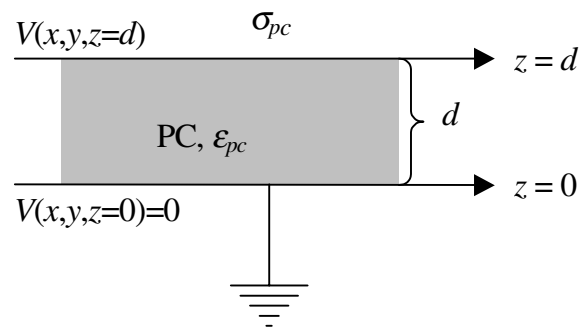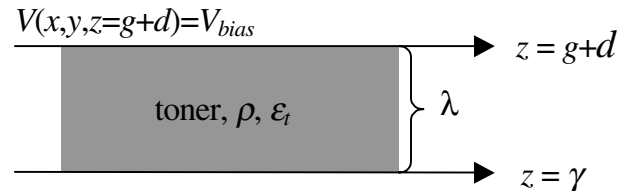

Figure 1. PC in the presence of toner and developer. In our model we assume piecewise-constant toner density distributions in the gap

Field Calculation

Initially, when the PC is exposed by the beam, the exposed region is far away from the developer where the toner resides. In this case, Laplace's equation is solved to

determine the voltage since there is no charge within the gap. The surface potential obtained in the previous section is used as a boundary condition. After the exposure, the PC drum rolls towards the developer, and eventually, the pattern will lie directly underneath the developer, as illustrated in Figure 1. In this case of a finite gap, we solve Poisson's equation to account for the effect of the developer bias and toner at the developer. Both Laplace's and Poisson's equations are solved by taking the 2D Fourier transform in the *x-y* plane and applying the boundary conditions. The field equations from these two cases are combined via Gauss's law, resulting in an expression for the field in the presence of the developer in terms of the "open space" surface potential from the PIDC data.

From the geometry in Figure 1, Poisson's equation can be written as

$$\left(\frac{\partial^2}{\partial x^2}+\frac{\partial^2}{\partial y^2}+\frac{\partial^2}{\partial z^2}\right)V(x,y,z)=$$
$$-\frac{\sigma_{PC}(x,y)}{\varepsilon_0\varepsilon_{PC}}\delta(z-d) \tag{1}$$
$$-\frac{\rho}{\varepsilon_0\varepsilon_t}\left[u(z-\gamma)-u(z-[g+d])\right]$$

where u is the unit step function, δ is the Dirac delta function, g is the developer gap length, d is the PC layer thickness, ρ is the toner charge density, σ_{PC} is the unknown PC charge density, and ε_t and ε_{PC} are the dielectric constants of toner and PC, respectively. Taking the negative gradient of the potential in Eq. (1), we obtain

$$E_z(k_x,k_y,z)$$
$$=\varepsilon_{PC}k_u\coth(k_u d)T_1(k_u,z)V_{PC}(k_x,k_y)$$
$$+k_u\left(\frac{V_{bias}}{\sinh(k_u g)}+\frac{\rho[\cosh(k_u\lambda)-1]}{\varepsilon_0\varepsilon_t k_u^2\sinh(k_u g)}\right)T_1(k_u,z)\delta(k_x,k_y), \tag{2}$$
$$-k_u\left(\frac{V_{bias}}{\sinh(k_u g)}+\frac{\rho[\cosh(k_u\lambda)-1]}{\varepsilon_0\varepsilon_t k_u^2\sinh(k_u g)}\right)\times$$
$$\cosh[k_u(z-d)]u(z-d)\delta(k_x,k_y)$$
$$+\sinh(k_u[z-\gamma])u(z-\gamma)\frac{\rho}{\varepsilon_0\varepsilon_t k_u}\delta(k_x,k_y)$$
$$-\sinh(k_u[z-(g+d)])u[z-(g+d)]\frac{\rho}{\varepsilon_0\varepsilon_t k_u}\delta(k_x,k_y)$$

$$E_x(k_x,k_y,z)=jk_x\varepsilon_{pc}\coth(k_u d)\,T_2(k_u,z)V_{PC}(k_x,k_y), \tag{3}$$

and

$$E_y(k_x,k_y,z)=jk_y\varepsilon_{pc}\coth(k_u d)\,T_2(k_u,z)V_{PC}(k_x,k_y), \tag{4}$$

where k_x and k_y are the spatial frequency variables in the *x*- and *y*- directions, respectively,

$$k_u=\sqrt{k_x^2+k_y^2}\,, \tag{5}$$

$$T_1(k_u,z)=\frac{\sinh(k_u(g+d))\cosh[k_u(z-d)]u(z-d)}{(\varepsilon_{PC}-1)\cosh(k_u d)\sinh(k_u g)+\sinh(k_u(g+d))}\,, \tag{6}$$
$$-\frac{\sinh(k_u g)\cosh(k_u z)}{(\varepsilon_{PC}-1)\cosh(k_u d)\sinh(k_u g)+\sinh(k_u(g+d))}$$

and

$$T_2(k_u,z)=\frac{\sinh(k_u(g+d))\sinh[k_u(z-d)]u(z-d)}{(\varepsilon_{PC}-1)\cosh(k_u d)\sinh(k_u g)+\sinh(k_u(g+d))}\,. \tag{7}$$
$$-\frac{\sinh(k_u g)\sinh(k_u z)}{(\varepsilon_{PC}-1)\cosh(k_u d)\sinh(k_u g)+\sinh(k_u(g+d))}$$

The fields in the spatial domain are obtained by taking the inverse Fourier transform of Eqs. (2)-(4). Note that the configuration in Figure 1 can be easily modified to model toner clouds[6] or toner anywhere in the gap.

Simulation

In this section, we present simulation results using the parameters listed in Table 1. As mentioned in an earlier section, exposure can be calculated analytically and we used the PIDC curve shown in Figure 2 to obtain the PC surface potential from the exposure. The normal field at the PC surface ($z = d$) using a 20 pixel × 20 pixel square is shown in Figure 3. The cross sections of the normal field along the *x*-axis at 0, 50, and 100 μm above the PC surface are shown in Figure 4. The fringe field around the boundary weakens as *z* gets closer to the developer. Figure 5 illustrates the *horizontal* field at 0, 50, and 100 μm above the PC surface.

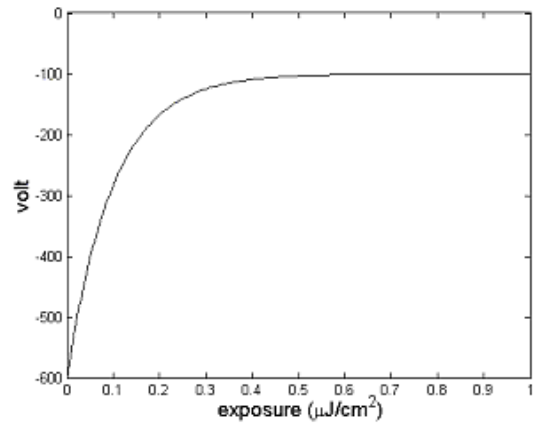*Figure 2. PIDC curve for example print engine*

Table 1. Virtual examples of printer parameters

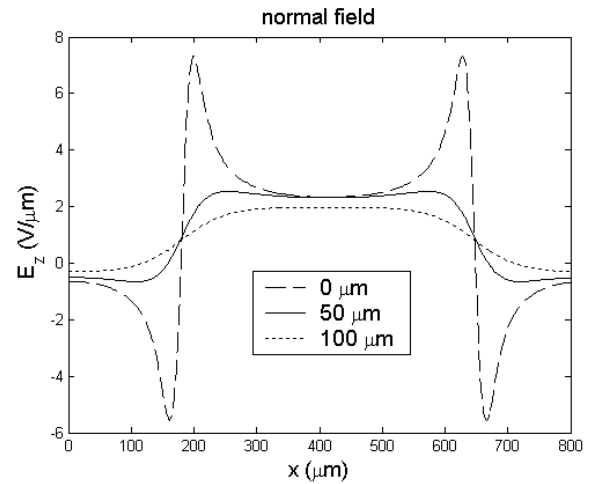|	
g developer gap	200 μm
λ toner layer thickness	50 μm
d PC thickness	20 μm
ρ toner charge density	-7 μC/cm^3
ε_t toner dielectric constant	3
ε_{PC} PC dielectric constant	3
V_{bias} developer bias	-200 V
V_{light} light voltage	-100 V
V_{dark} dark voltage	-600 V
t_{rise} laser beam risetime	2 ns
t_{fall} laser beam falltime	2 ns
P laser power	0.05 mW
v_{scan} laser scan velocity	500 m/s
α laser spot parameter	20 μm
β laser spot parameter	20 μm
r printer resolution	1200 dpi

Figure 4. Normal field at 0, 50, and 100 μm above the PC surface
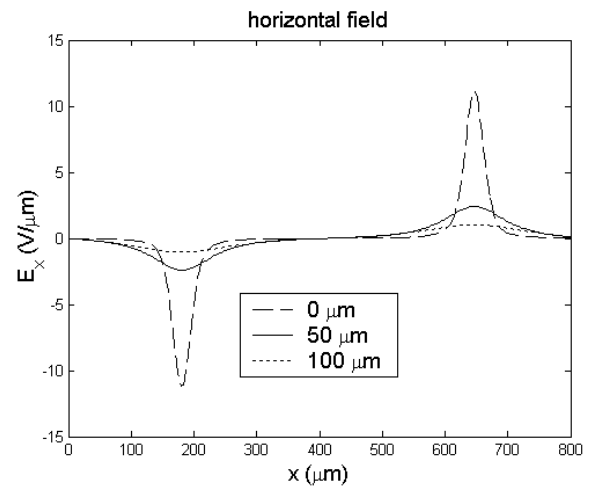
Figure 5. Horizontal field at 0, 50, and 100 μm above the PC

Figure 3. Normal field at the PC (20 pixels × 20 pixels)
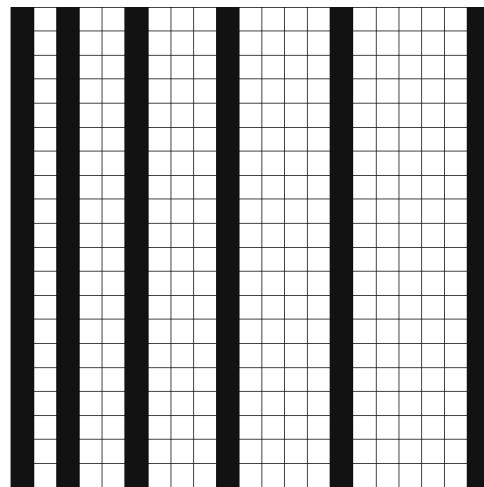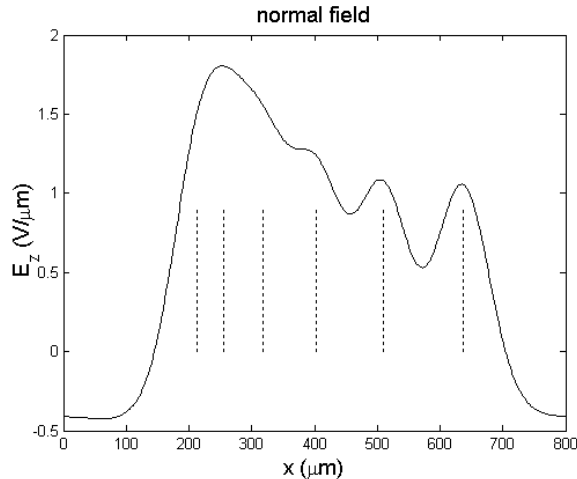

Figure 6. Input bitmap
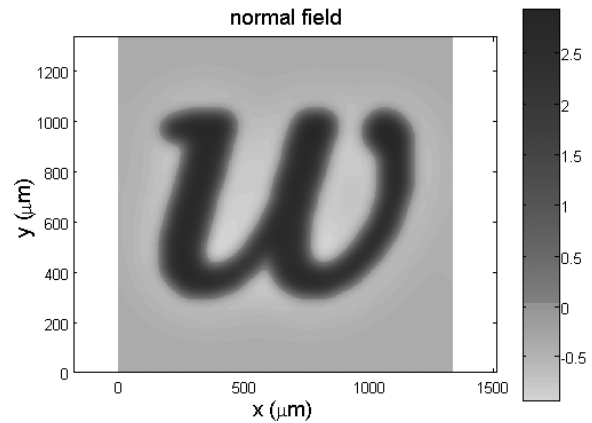
Figure 7. Normal field using the bitmap in Figure 6

Figure 9. Normal field of the "w" character

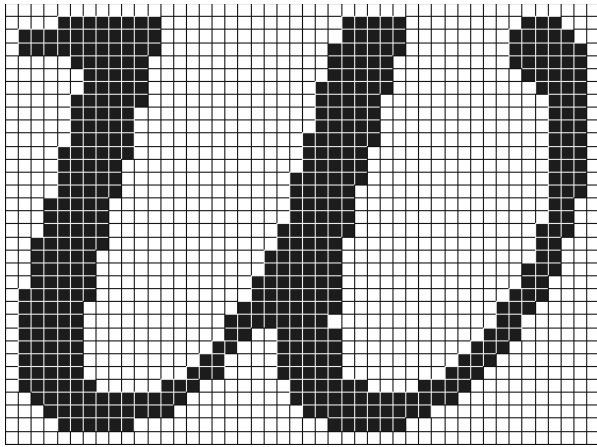*Figure 8. A 4-point "w" character*

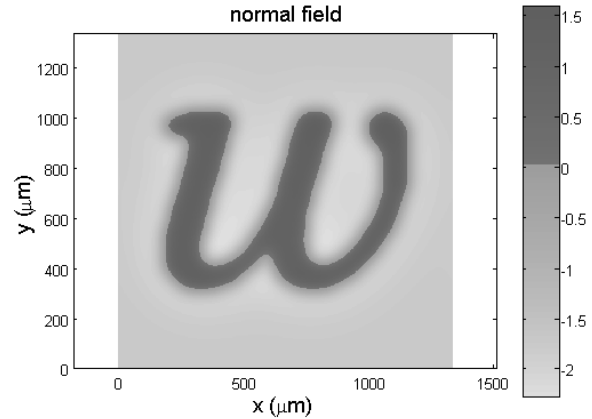*Figure 10. Normal field when λ = 20 μm*

Our field calculation method works for any input pattern, no matter how complicated it may be. Consider the bitmap shown in Figure 6. The normal field at 70 μm above the PC is shown in Figure 7, where the dotted lines correspond to the positions of the six lines in Figure 6. Note that the first three lines are completely merged together, forming a single wider, darker line, while the other lines result in partial overlapping. The field plot readily demonstrates the effect and extent of dot-overlapping. Hence, lines can be strategically positioned to take advantage of this effect. Figure 9 shows the normal field at 50 μm above the PC surface using the 4-point "w" character in Figure 8. The parameters listed in Table 1 are intimately coupled with one another. Changing the values of the parameters often results in a noticeable change in field. For example, when the initial toner layer thickness, λ, (see Figure 1) is changed from 50 to 20 μm, the width of the "w" becomes more narrow, as illustrated in Figure 10.

Conclusion

We introduced a novel field calculation technique for obtaining the electric field in the developer gap. It uses a set of physical printer parameters to compute the exposure energy on the photoconductor surface, and the corresponding photoconductor surface potential is obtained from the Photo-Induced Discharge Characteristics (PIDC) of the photoconductor. The surface potential is then used as a boundary condition for solving Poisson's equation. The normal and horizontal fields are subsequently obtained by taking the negative gradient of the voltage. Initially, when the PC is exposed by the beam, the exposed region is far away from the developer where the toner resides, and the PC drum rolls towards the developer. Eventually, the pattern lies directly underneath the developer. The field equations from these two cases are combined via Gauss's law, resulting in an expression for the field in the presence of the developer in terms of the surface potential in the

absence of the developer. This method accounts for dot-overlapping, allowing field calculation anywhere in the gap for an arbitrary input bitmap. We demonstrated that the field of any bitmap can be readily calculated and how our field model can be utilized to exploit dot-overlapping.

Acknowledgement

References

1. E. M. Williams, *Photographic Science and Engineering*, vol. **26**, no. 2, pg. 88-91 (1982).
2. Cheng C. Kao, *J. Appl. Phys*., vol. **44**, no. 4, pg. 1543-1551 (1973).
3. H. E. J. Neugebauer, *Applied Optics*, vol. **3**, no. 3 (1964).
4. E. M. Williams, The physics and technology of xerographic processes, Krieger Publishing Company, Malaba, Florida, 1993.
5. J. Yi, "A xerographic simulation model," M. S. Thesis, University if Idaho, Moscow ID (1999).
6. J. Yi et al., Gray Level and DMA Estimation in Monocomponent Development Systems, *Proc. NIP18,* p. 726 (2002).

Biography

Jang Yi received his B.S. degree in computer engineering from the University of Idaho in 1997 and a M.S. degree in electrical engineering in 1999. He's currently a Ph.D student at the same institute. His thesis was on designing an electrophotographic simulation tool. His current research area is the development process.